Heat transfer enhancement during freezing process of Nano Phase Change Material (NPCM) in a spherical capsule

R.Y. Sakr, Ahmed A.A. Attia *, Ahmed A. Altohamy, Ismail M.M. Elsemary, M.F. Abd Rabbo

Mechanical Engineering Department, Benha University, Shoubra Faculty of Engineering, 108, Shoubra Street, Cairo, Egypt

HIGHLIGHTS

- Dimensional analysis for freezing process of nano phase change material (NPCM).
- Stefan, Grashof and Reynolds number previously used in melting of NPCM.
- Useful empirical correlations are obtained and can be helpful in practice.

ARTICLE INFO

ABSTRACT

An investigation on performance of Nano Phase Change Material (NPCM) (water as PCM and 50 nm Al_2O_3) in a spherical capsule is carried out. Both the inlet temperature and volume flow rate of heat transfer fluid (HTF) (Aqua-ethylene glycol solution is used as a HTF) are varied to maintain the capsule wall temperature constant at a temperature range from $-4\,°C$ to $-10\,°C$ respectively. The volume fraction concentration of the nanoparticles in the used PCM in the experiment ranges from 0.5% to 2%. The results is presented in the form of relations between the solidified mass fraction, percentage of thermal energy storage and the average Nusselt number versus an appropriate combination of Fourier, Stefan, and Rayleigh numbers as well as the volume fraction of nanoparticles. The dimensional analysis that is presented here results a number of useful empirical correlations that can be used in practice.

© 2017 Elsevier Ltd. All rights reserved.

1. Introduction

Global warming causes a widespread use of refrigeration and air conditioning utilities especially in the developing countries. The load of these utilities is characterized by its variable nature. So, the electric power demand is of daily and seasonal fluctuations causing a gap between the demand and supply of energy. Cool Thermal Energy Storage (CTES) systems seem to be one of the most appropriate methods to bridge the gap between the demand and supply of the energy. The application of CTES systems offers a potential for substantial cost saving by using the off-peak electricity to produce coolness in a certain medium. There are two types of CTES systems one is called sensible cool storage and the other is called latent cool storage. The basic concept of the encapsulated thermal energy storage air conditioning system is utilizing the characteristics of the phase change material (PCM) packed inside capsules stored in a tank. These capsules release or absorb a great amount of latent heat during phase change process.

Eames and Adref [1] described and evaluated the results of an experimental study on the characterization of freezing and melting processes of water contained in a spherical capsule. Their results include semi-empirical equations that predict the mass of ice within the sphere at any time during the freezing or melting process.

Cheralathan et al. [2] carried out an experimental investigation on the thermal performance of an industrial refrigeration system integrated with encapsulated PCM during charging process. They reported that a 1 °C decrease in the evaporator temperature results in 3–4% increase in the specific energy consumption and 1 °C decrease in condensing temperature leads to 2.25–3.25% decrease in specific energy consumption.

Bedecarrats et al. [3] conducted a series of experiments and reported that when a charge mode follows an incomplete discharge mode, the charge mode is the result of the crystallization of some capsules with super cooling and the remaining without super cooling. The consequence is that the charge mode is made at a higher temperature with a relatively shorter duration.

* Corresponding author.
  E-mail addresses: Ahmed_attia72@yahoo.com, Ahmed.attia@feng.bu.edu.eg
(A.A.A. Attia).

Nomenclature

A_S	sphere surface area, m^2
A, B	correlations coefficients, –
c	specific heat, J/kg K
Fo	Fourier number, –
g	gravity acceleration = 9.8 m/s^2
H	vertical distance, measured from the center of the spherical capsule to the free surface of the encapsulated PCM, m
h	convective heat transfer coefficient, W/m^2 K
k	thermal conductivity, W/m·K
L	latent heat of fusion of water, kJ/kg·K
m_o	mass of PCM encapsulated inside the spherical capsule, kg
m_s	solidified mass, kg
Nu	Nusselt number
Q	thermal energy stored, W
q_{ins}	instantaneously surface heat flux
R	sphere radius, m
Ra	Rayleigh number
$r_{avg_{h,v}}$	average radius of solid–liquid interface, m
r_h	horizontal radius of solid–liquid interface, m
r_{in}	inside radius of test capsule, m
r_v	vertical radius of solid–liquid interface, m
Ste	Stefan number, –
SF	solidified mass fraction, –
T	temperature, °C
t	time, s
V_{shell}	solidified shell volume, m^3
V_{PCM}	phase change material volume, m^3
v	HTF velocity, m/s

x	volume fraction, –
z	mass fraction, –
Al_2O_3	aluminum oxide
lpm	liter per minute
CuO	copper oxide
TiO_2	titanium oxide

Greek symbols

β	volumetric expansion coefficient, 1/K
Δ	difference
μ	dynamic viscosity, kg/m·s
ρ	density, kg/m^3

Subscripts

l	liquid
np	nano particles
PC	phase change
s	solid
S	surface
st	stored
w	water
i	ice

Abbreviations

PCM	Phase Change Material
HTF	Heat Transfer Fluid
NPCM	Nano Phase Change Material
CTES	Cool Thermal Energy Storage
LDPE	Low Density Polyethylene

Eames and Adref [4] concluded that 90% of the cold could be extracted from spherical capsules with 70% of the time required to discharge it completely.

Ismail et al. [5] conducted a numerical study and reported the results of their study on the heat transfer process for the solidification of water inside a spherical capsule. Their numerical results were validated by comparison with experimental results realized by the authors.

Chan and Tan [6] carried out an experimental study on solidification inside a spherical enclosure. They concluded that the temperature difference between the HTF and PCM has the major influence on the solidification process while the effect of initial liquid superheats is insignificant.

Ismail and Moraes [7] conducted an experimental and numerical study on the solidification of different PCMs encapsulated in spherical shells. They concluded that increasing the diameter of the spherical shell is found to increase the time for complete solidification. This increase in complete charging time is relatively small up to 0.076 m diameter where the conduction is the dominant mode of heat transfer. As the diameter increases, convection in the liquid region becomes stronger and causes the liquid to move away from the solidification front, so the time for complete solidification increases; i.e. natural convection retards the freezing process.

ElGhanam et al. [8] reported the results of an experimental study on the heat transfer during freezing and melting (cool energy charging/discharging) of water inside a spherical capsule of different materials and sizes. A mixture of water with 35-wt% ethylene glycol (aqua solution) was used as HTF. The effects of the volume flow rate and the inlet HTF temperature as well as the capsule material and size on the time for completing charging/discharging, solidified/melted mass fraction, charging/discharging rate, energy stored/regain and the energy recovery ratio were investigated.

Nowadays, due to rapid advancement in the field on nanotechnology, a new concept of dispersing nanoparticles with base PCM was attempted by the researchers to improve the thermal properties of the materials which called NPCMs.

Wu et al. [9] conducted an experimental study and reported that the addition of Al_2O_3-H_2O nanoparticles remarkably decreases the super cooling degree of water, advances the beginning of freezing process and reduces the total freezing time. They also reported that the total freezing time can be reduced by 20.5% by adding 0.2 wt% of Al_2O_3-H_2O nanoparticles.

Kumaresan et al. [10] represented the solidification behavior of water based Nano fluid phase change material encapsulated in a spherical container. The Nano fluid phase change material was prepared by dispersing the multiwall carbon nanotube in deionized water as the base PCM. Maximum reductions of 20% were observed in the solidification time with NFPCM (Nano fluid phase change material.

Chandrasekaran et al. [11] investigated the solidification characteristics of water based NPCM. The NPCM was prepared by dispersing nanoparticles of copper oxide and a nucleating agent in the base fluid inside a spherical capsule. A significant reduction in solidification time of was about 35%. Also, they found that the presence of nucleating agent eliminated the problem of sub cooling in the PCM.

The heat transfer characteristics and thermal storage performance of enhanced neopentyl-glycol NPG in a cylindrical container are investigated numerically by Elsayed [12]. Best performance in heat storage is achieved by the volume fraction of (6% Al + 3% SiO_2+3% TiO_2) with NPG compared to the other compositions.

Altohamy et al. [13] studied experimentally the charging process of cool thermal energy storage system. Experiments were carried out using water base Nano fluid (50 nmAl$_2$O$_3$) phase change material contained in a spherical capsule with volume fraction ranged from 0.5% to 2%. The results showed that the max percentage reductions in complete charging time is 32%. Attia el al. [14] concluded that dispersing Al$_2$O$_3$ nanoparticles in water as phase change material is more benefit than dispersing them into aqua solution of ethylene glycol, as NHTF in charging process of CTES system in a spherical capsule.

It has been observed from the available literature that the addition of Nano particles enhances the heat transfer process, especially during freezing along with a significant reduction in the time of process completion. Also, it is found that only limited research works are being reported on the freezing of water as a base fluid of PCM with the dispersion of metal or metal oxide nanoparticles. The urgent need to design and develop an efficient CTES system through enhanced heat transfer rate and minimum complete charging time directed the authors' objectives to explore the freezing behavior and heat transfer characteristic using pure water as PCM and as NPCM with dispersing Al$_2$O$_3$ nanoparticles up to 2% volume fraction in a spherical capsule.

Also, there is a need to quantify the freezing and the heat transfer characteristics by deducing empirical correlations for the solidified mass fraction, percentage of thermal energy stored as well as the surface average Nusselt number in terms of the dimensionless groups that govern the freezing phenomenon including the volume fraction of the dispersed nanoparticles. This empirical formula will be helpful in design and evaluation process for the cool storage systems.

2. Experimental description

The experimental test rig is illustrated schematically in Fig. 1. The test rig consists of a refrigeration cycle working with R404A, which is used to cool aqua solution of ethylene glycol with a concentration of 30% by weight having a freezing point of −15 °C. This solution is considered as the heat transfer fluid which adds or removes heat from (distilled water) phase change material that is contained in the spherical capsule (test section).

Two identical cylindrical tanks with end top and bottom caps having a diameter of 200 mm and a height of 900 mm were used as charging and discharging spaces. Each tank was wrapped with a layer of 50 mm thickness glass wool insulation to reduce the heat gain from surrounding and was filled up to 95% of its volume with the HTF. The bottom of the two tanks has a conical shape to ensure no settlement of the nanoparticles.

A low-density polyethylene spherical capsule with inner and outer diameters of 80 and 84 mm respectively was filled with 80% of its inner volume with a PCM to avoid damage of thermal expansion during the solidification process. Eleven calibrated Copper-Constantan (T-type) thermocouples were employed to measure the temperature distribution with ±0.5 °C as depicted in Fig. 2.

A centrifugal pump is used to circulate the HTF through the piping system to carry out the charging and discharging process of the experiments.

A data acquisition card (NI USB-6210, 32-inputs, having resolution of 16-bit and scanning rate of 250 kS/s) is used to record the temperature readings through the thermocouples. The volume flow rate of HTF is monitored by using a calibrated rotameter and controlled via a manual gate valve. ELIWELL IC 901, 0.5% accuracy, and 1 °C set-point differential digital temperature controller is used to control the required temperature inside the charging or discharging tank during the charging and discharging experiments. A series of charging experiments were performed under different operating conditions.

In the charging process, the refrigeration unit operates to cool the circulating HTF. The digital temperature controller is adjusted at one of the four test temperatures as listed in Table 1. Once the adjusted HTF temperature is reached, the volume flow rate of the HTF is set at one of the different volume flow rates listed in Table 1. Then the capsule is immersed in of the charging tank. Both the HTF temperature and flow rate control results in a nearly constant capsule wall temperature ranged from −4 °C to −10 °C. The measurements of the PCM temperatures inside the test section and the HTF

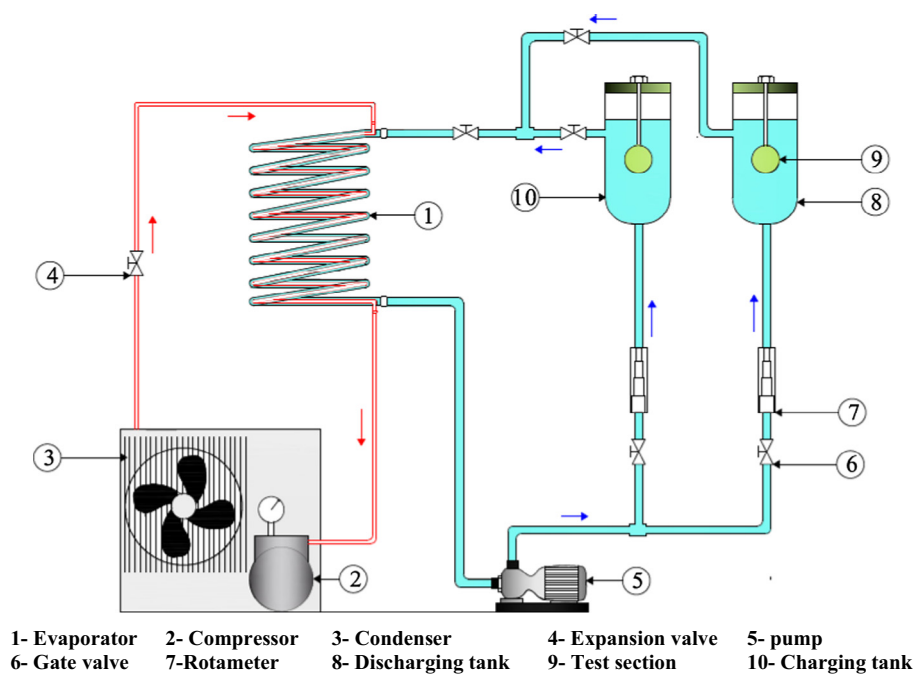| 1- Evaporator | 2- Compressor | 3- Condenser | 4- Expansion valve | 5- pump |
| 6- Gate valve | 7-Rotameter | 8- Discharging tank | 9- Test section | 10- Charging tank |

Fig. 1. Schematic diagram of the experimental test rig.
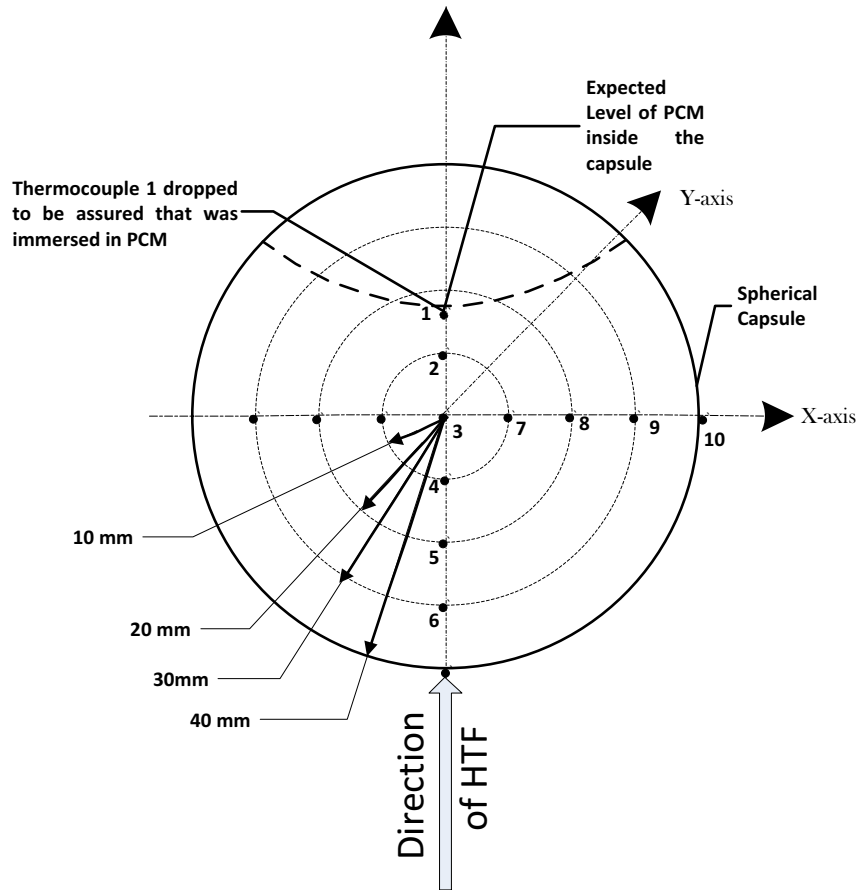
Fig. 2. Thermocouples distribution inside PCM Capsule.

Table 1
Experimental conditions.

Capsule surface temperature	Capsule surface temperature (during charging process) ranged from −4 °C to −10 °C due to maintaining the heat transfer fluid; HTF; (Aqua ethylene glycol solution) at −6, −8, −10 °C and −12 °C and volume flow rates: 6.0, 8.0, 10.0, and 12.0 LPM
PCM	Water + Al_2O_3 nanoparticles with volume fraction of 0%, 0.5%, 1.0%, 1.5% and 2.0%

temperatures around it were scanned and recorded every one second. As the thermal equilibrium between the PCM and HTF is reached the experiment is terminated.

3. Nano fluid preparation

The particles used in the nano fluid experiments are gamma-alumina (γ-Al_2O_3) nano powders, 50 nm average particle size with

Table 2
Results of Uncertainty Analysis.

Parameter	Relative uncertainty	Parameter	Relative uncertainty
Temperature	±0.7%	Rayleigh number	±0.53%
Encapsulated volume (V_o)	±0.33%	Fourier number	±0.9%
Solidified mass fraction (m_s)	±1.12%	Stefan number	±2.02%
Surface heat flux (q_{ins})	±1.9%	Heat stored	±3%
Latent heat	±1.5%	Nusselt number	±3.8%

Table 3
Properties of γ-Al_2O_3 nanoparticles.

Thermal conductivity ($W/m \cdot °$ C)	Density (kg/m^3)	Specific heat ($J/kg \cdot °$ C)
36	3600	773

surface area >200 m^2/g). The thermo physical properties of γ-Al_2O_3 nanoparticles are revealed in Table 3.

The γ-Al_2O_3/water Nano fluid was prepared in this study with four different nanoparticles volume concentrations of 0.25%, 0.5%, 0.75% and 1.0%. The dispersion of particles in water was done in two step the first step is putting the mixture in ultra-sonication for 90 min in an EG bath temperature of 30 °C. The second steps to achieve good mixing for the nano fluid the mixture was pumped in the tube coil for six hours before beginning the experiments.

4. Data reduction

The spherical capsule that will be used in the present work is filled with NPCM up to 80% of its internal volume see Fig. 2. the capsule was positioned in middle of the charging tank. So the flow of the HTF around the sphere is assumed to be symmetric. The thermocouples were placed in the specified places in the capsule to track the temperature changes through the solidification process. This will be used to determine the solidified mass fraction of NPCM inside the capsule through the test by getting r_h, r_v then getting $r_{avgh,v}$ and finally get the solidified mass fraction at any time through the experiment, [8]. Based on, a symmetric solidified

shell is expected to be exists, and with the outputs of the data acquisition system for each experiment at different concentrations of nanoparticles used; the following equations can be applied.

$$V_{shell} = (2/3)\pi(r_{in}^3 - r_{avg_{h,v}}^3) + \pi H(r_{in}^2 - r_{avg_{h,v}}^2) \qquad (1)$$

where $r_{avg_{h,v}} = (r_h + r_v)/2$

The solidified mass is calculate as

$$m_s = \rho_i * V_s \qquad (2)$$

The solidified mass fraction is calculated from

$$SF = m_s/(\rho_w * V_o) \qquad (3)$$

where The NPCM volume, $V_O = 0.80\, V_{capsule}$.

The accumulative thermal energy stored with the capsule is given by:

$$Q_{st} = \rho_w V_o \left\{ c_w(T_o - T_I) + \frac{m_s}{m_o}(L) + \frac{m_s}{m_o} c_i(T_{PC} - T_s) \right\} \qquad (4)$$

The percentage of the thermal energy stored is calculated as:

$$\% \, CTES = Q_{st}/Q_{st,max} \qquad (5)$$

The surface heat flux,

$$q_S = \Delta Q_{st}/(A_S \Delta t) \qquad (6)$$

where $A_S = 4\pi R^2$

The heat transfer coefficient, h is given by

$$h = \frac{q_S}{\Delta T} \qquad (7)$$

where $\Delta T = T_S - T_{PC}$,

T_S: is the surface capsule temperature,

T_{PC}: is the phase change temperature.

The following non-dimensional parameters were presented to evaluate the effect of nanoparticles addition to PCM on the thermal behavior of melting process [15,16]. These parameters can be applied to analyze the NPCM freezing process in the present experimental work.

$$\text{Stefan number, Ste} = c_{NPCM} * (T_S - T_{PC})/L \qquad (8)$$

$$\text{Rayleigh number, Ra} = \frac{\rho_{NPCM} g\beta(T_S - T_{PC})R^3}{\mu_{NPCM}\alpha_{NPCM}} \qquad (9)$$

$$\text{Fourier number, Fo} = \frac{k_{NPCM}t}{(\rho c)_{NPCM}R^2} \qquad (10)$$

Nanoparticles mass fraction concentration

$$z = m_{np}/(m_{np} + m_{NPCM}) \qquad (11)$$

Nusselt number

$$Nu_{NPCM} = \frac{hR}{k_{NPCM}} \qquad (12)$$

The properties of the NPCM that used in the calculation of the performance parameters were calculated based on the assumption of two-component mixture model of the pure PCM and nanoparticles material. The effective properties NPCM are calculated as follows:

The effective density:

$$(\rho)_{NPCM} = (1 - x)\rho_{PCM} + x\rho_{np} \qquad (13)$$

x: is the volume fraction of nanoparticles and is given by:

$$x = \frac{Z\rho_{PCM}}{Z\rho_{PCM} + (1 - Z)\rho_{np}} \qquad (14)$$

where z: mass fraction percentage of nanoparticles.

The effective specific heat:

$$(\rho c)_{NPCM} = (1 - x)(\rho c)_{PCM} + x(\rho c)_{np}, \qquad (15)$$

The effective thermal conductivity is given by the Maxwell model [16], as:

$$k_{NPCM} = k_{PCM} \frac{k_{np} + 2k_{PCM} - 2x(k_{PCM} - k_{np})}{k_{np} + 2k_{PCM} + x(k_{PCM} - k_{np})} \qquad (16)$$

The effective viscosity is given by Brinkman correlation [16] as:

$$\mu_{NPCM} = \mu_{PCM}(1 - x)^{-2.5} \qquad (17)$$

5. Results and discussion

The solidified mass fraction, the percentage of thermal energy cool storage, Nusselt number and complete charging time of the freezing process are chosen to express the freezing behavior of both PCM and NPCM contained in the spherical capsule under all experiment conditions. Table 1 illustrates the experimental conditions.

Fig. 3, The solidified mass fraction with different values of Stefan number ranged from 0.05 to 0.113 and Rayleigh numbers ranged from 5.12×10^7 to 1.35×10^8; corresponding to surface temperature of $(-4\,°C, -6\,°C, -8\,°C, -9\,°C)$; is depicted in Fig. 3. It can be concluded from the figure that higher freezing rate at the beginning of the freezing process, then it decreases as the solidified PCM (ice) layer increases resulting in an increase of the conduction thermal resistance. Also, as the Stefan and Rayleigh numbers increase the solidified mass fraction increases as they express the temperature difference and buoyancy driving force for the heat transfer process. The temporal variation of the solidified mass fraction for different values of Rayleigh and Stefan numbers for NPCM having a volume fraction of nanoparticles of 2% is also depicted. It is illustrated also that the addition of nanoparticles accelerates the process of freezing as the rate of freezing increases and the time for complete freezing is reduced. Also, from the figure it is observed that an average percentage of 35% increase in the solidified mass fraction due to the increase of Rayleigh number from 5.12×10^7 to 1.35×10^8 for $Fo \leq 0.4$ where the solidified fraction ranged from 70% to 98%. The effect of volume fraction of the added nanoparticles to the PCM on the behavior of freezing process for $Ra = 1.33 \times 10^8$ and $Ste = 0.116$ corresponding to surface capsule temperature of $-9\,°C$ is illustrated. The temporal variation of the solidified mass fraction of NPCM for different values of volume fraction of nanoparticles is shown. It is observed from the figure that as the value of volume fraction of nanoparticles increases the solidified mass fraction increases and this may be due to the enhancement of the thermal properties of the NPCM. Also, an average percentage increase of solidified mass fraction of 23% for $Fo \leq 0.3$ due to adding 2% by volume of nanoparticles to the pure PCM.

A similar behavior of solidified mass fraction is noticed for the percentage of cool thermal energy storage in Fig. 4. this is may be due to the latent heat of freezing which is considered to be the major part of the energy stored. It is noted that an average increase of the thermal energy cool storage by 30% due to the increase of Rayleigh number from 5.12×10^7 to 1.35×10^8 for $Fo \leq 0.3$ where the energy stored ranged from 77% to 93%. Also, the same behavior is noticed for the variation for the percentage of the thermal energy cool storage with time.

The variation of the average Nusselt number with the dimensionless time for different Rayleigh and Stefan numbers is represented in Fig. 5. It is observed that a sharp decrease in the
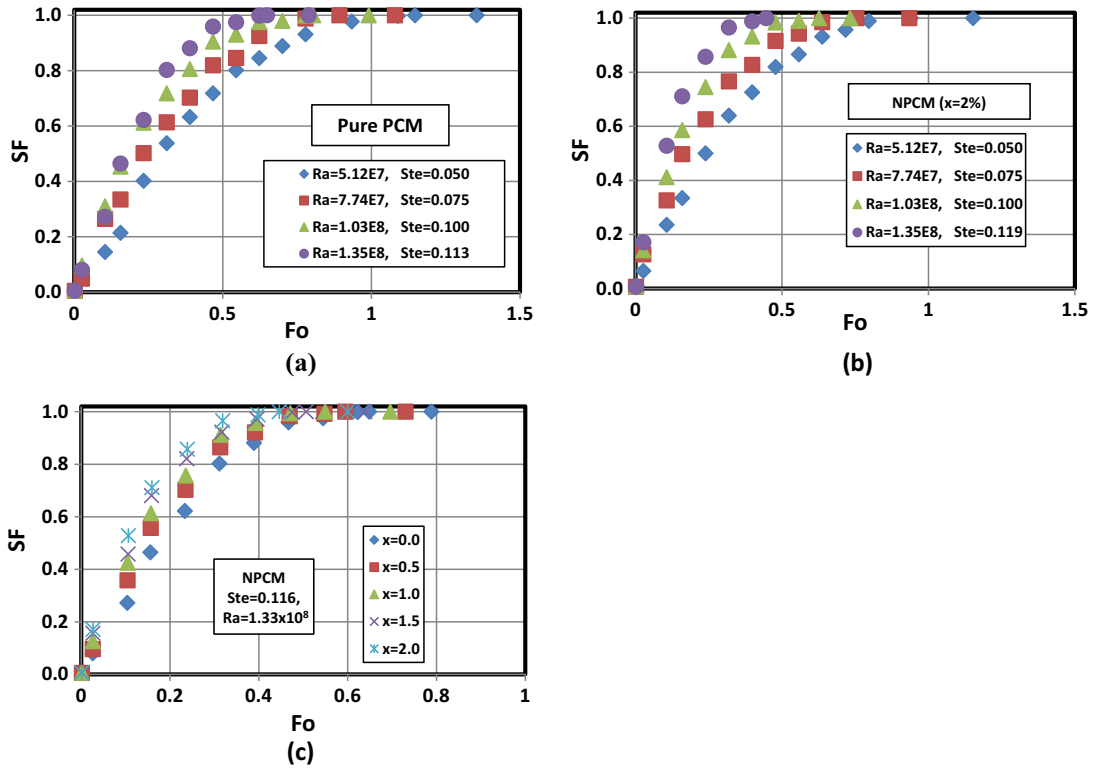
Fig. 3. Temporal variation of the solidified mass fraction for (a) pure PCM (b) NPCM for different Stefan and Rayleigh numbers at x = 2% and (c) for different concentration (Ste = 0.116, Ra = 1.33 × 10^8).
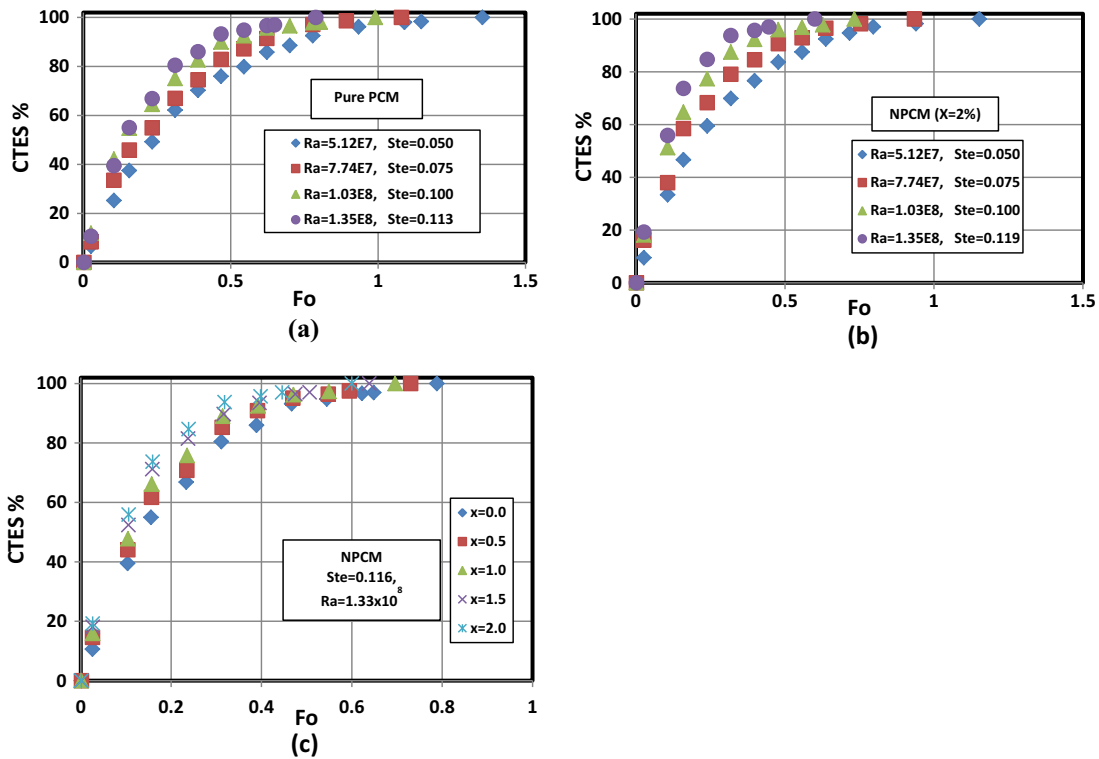

Fig. 4. Temporal variation of the heat stored percentage for (a) pure PCM (b) NPCM for different Stefan and Rayleigh numbers at x = 2% and (c) for different concentration (Ste = 0.116, Ra = 1.33 × 10^8).

average Nusselt number at the early stages of the freezing process then the value of Nusselt number approaches asymptotic value. Also, up to a certain value of Rayleigh number the Nusselt number has higher values for lower values of Rayleigh number and Stefan numbers. Beyond this value the Nusselt number is higher. This is may be due to change in the flow characteristics of the liquid
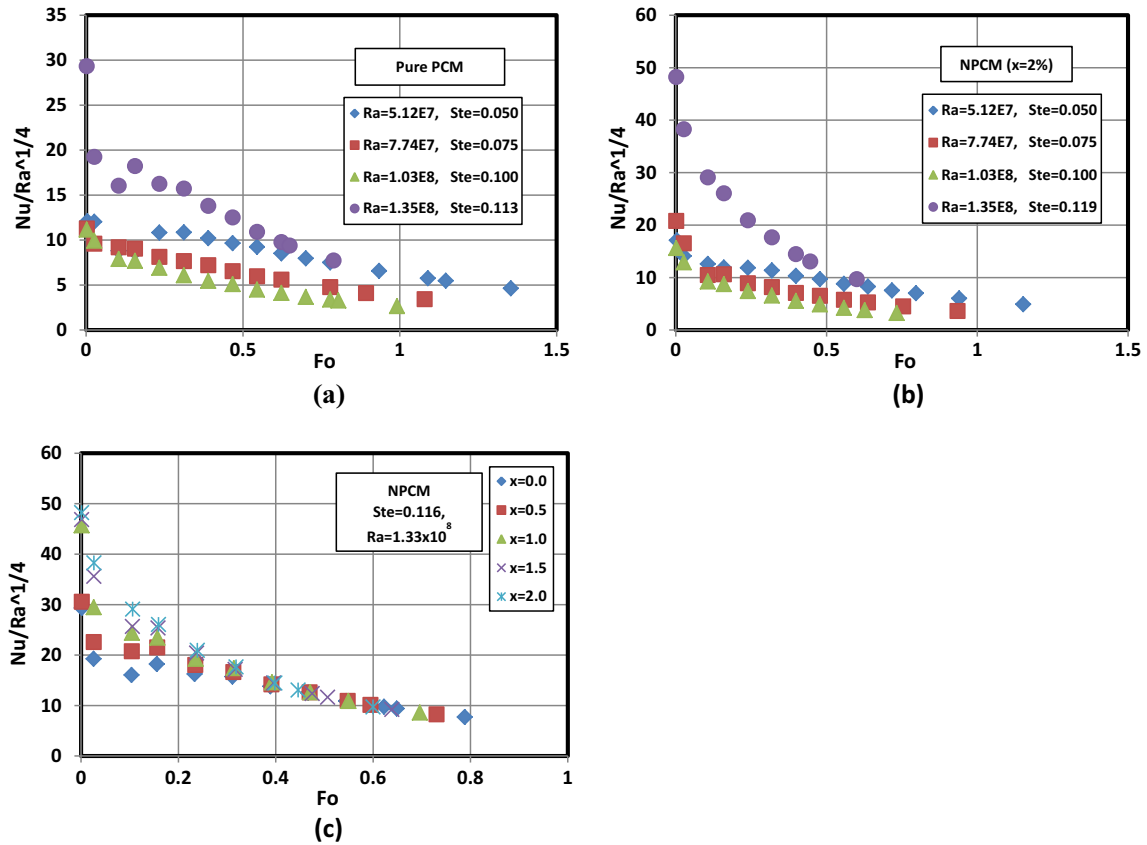
Fig. 5. Variation of the average Nusselt number with dimensionless time for (a) pure PCM (b) NPCM for different Stefan and Rayleigh numbers at x = 2% and (c) for different concentration (Ste = 0.116, Ra = 1.33×10^8).

phase. An average percentage reduction of 43% of the complete dimensionless charging time due to the increase of Rayleigh number by a percentage of 164% is noticed illustrated in Fig. 5. The variation of the average Nusselt number with the dimensionless time for different values of Rayleigh and Stefan numbers for NPCM of 2% volume fraction is represented also.

It is observed from the figure that the average Nusselt number decreases with time. Also, it is noticed that there is a significant variation in the value of Nusselt number at early stages of the freezing process due to the enhancement of the thermal properties of NPCM followed by the insignificant variation in the average Nusselt number and this may be due to the dominance of the convection heat transfer. The average Nusselt number decreases as the freezing process proceeds. Also, significant effect of the volume fraction of nanoparticles on the average Nusselt number at the early stages of the freezing process due to the enhancement of

thermal conductivity of the NPCM as the conduction is the dominant mode of heat transfer. This is followed by insignificant variation in the average Nusselt number with the volume fraction of nanoparticles added to PCM and this may be due to the increase of the conduction resistance.

The application of the dimensionless groups introduced in the previously described data reduction leads to the generalized results illustrated in Figs. 6–9 for pure PCM and NPCM.

Fig. 6 illustrates the solidified mass fraction for the pure PCM against a suggested combination of Fourier, Stefan and Rayleigh numbers group namely $FoSte^{1/3}Ra^{1/4}$ obtained for spherical capsules similar to that used in the literature for a melting process in a spherical capsule [15,16] except for replacing Grashof number in the literature by Rayleigh number in the present work. One can observe that all the data in the range of Ste and Ra can be represented by Correlation Eq. (18) in the following form:
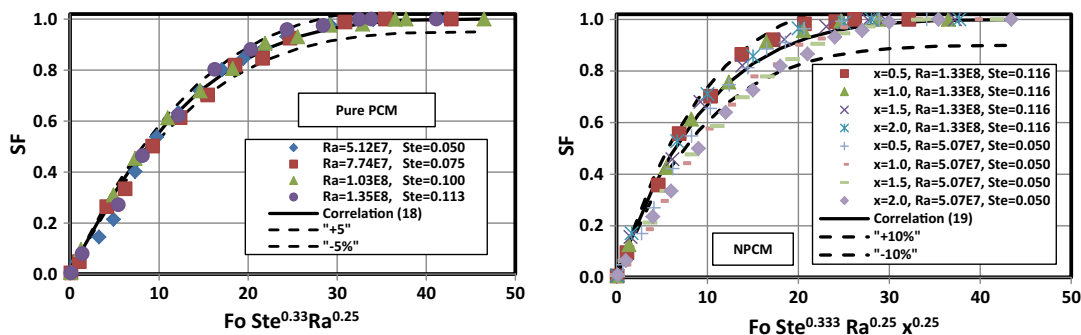

Fig. 6. Solidified mass fraction correlated to pure PCM and NPCM combination of dimensionless grouping.
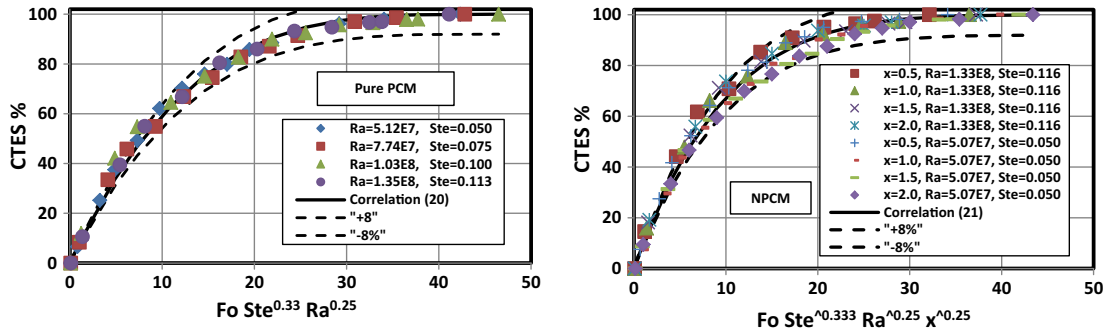
Fig. 7. Cool thermal energy storage percentage correlated to pure PCM and NPCM combination of dimensionless grouping.
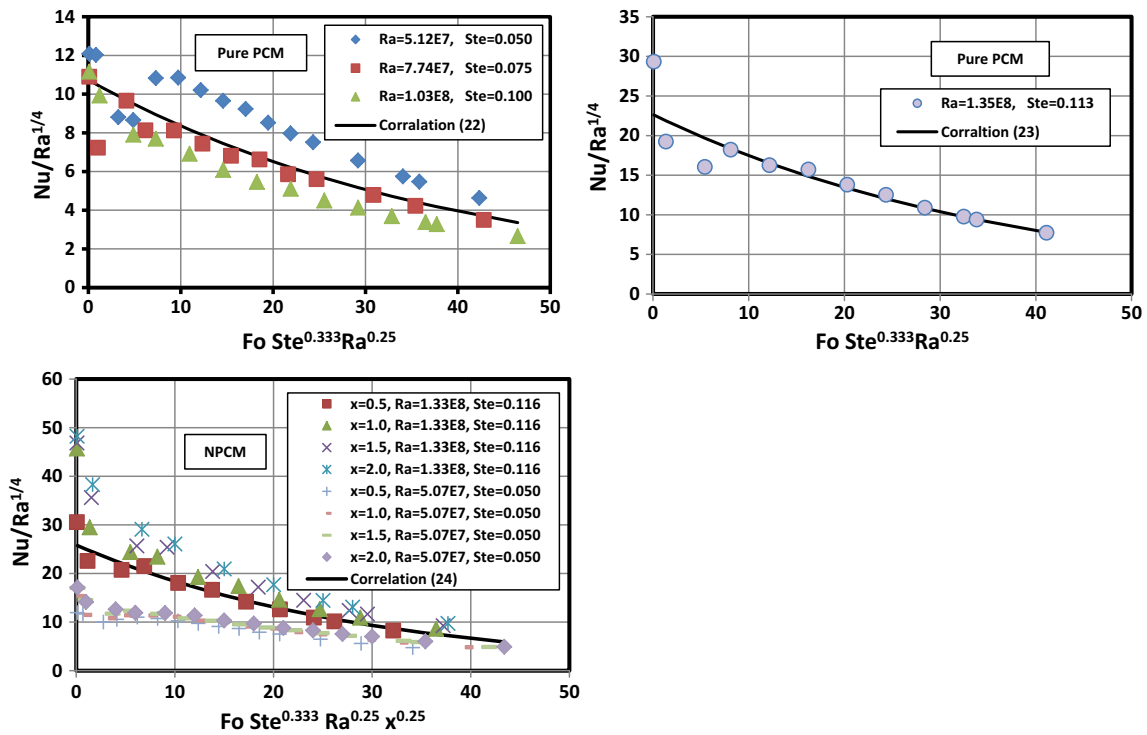

Fig. 8. Average Nusselt number correlated to Pure PCM and NPCM combination of dimensionless groupting.
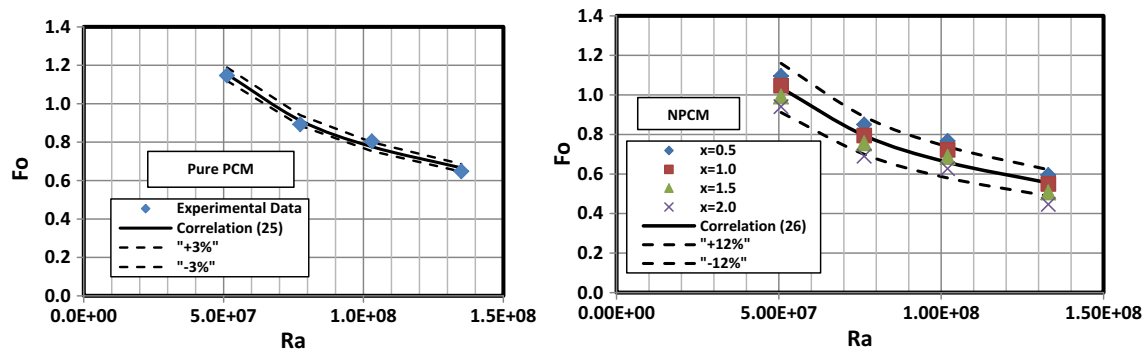

Fig. 9. Variation of complete charging dimensionless time with Rayleigh number for pure PCM and NPCM.

Table 4
Correlations constants and maximum percentage error.

Correlation No.	A	B	ε_{max}	Correlation No.	A	B	ε_{max}
19	48	3.5	±5%	23	42	6.25	±10%
20	47	3.75	±8%	24	43.5	6.5	±8%

$$SF = 1 - \left(1 - \frac{Fo\,Ste^{1/3}Ra^{1/4}}{A}\right)^{B} \qquad (18)$$

With a maximum deviation for the experimental data of ±5% is observed. The coefficients A and B are constants illustrated in Table 4.

The experimental data for NPCM is utilized to obtain correlation equations similar to that obtained for pure PCM. The only difference is the addition of the volume fraction of nanoparticles in NPCM to the dimensionless groups. The dimensionless group for correlations (23)–(25) is $FoSte^{1/3}Ra^{1/4}x^{1/4}$. The solidified mass fraction is correlated to the chosen dimensionless group and illustrated in Fig. 6 as:

$$SF = 1 - \left(1 - \frac{Fo\,Ste^{1/3}Ra^{1/4}x^{1/4}}{A}\right)^{B}. \qquad (19)$$

The percentage of thermal energy cool storage for pure PCM, TECS%, against the dimensionless group $FoSte^{1/3}Ra^{1/4}$ is depicted in Fig. 7. Correlation Eq. (20) with a maximum deviation of ±8% and represents nearly all of the experimental data and has the form of:-

$$TECS = 1 - \left(1 - \frac{FoSte^{1/3}Ra^{1/4}}{A}\right)^{B}\% \qquad (20)$$

And A, B are constants given in Table 4.

With a maximum deviation of ±10% and A and B are constants given in Table 4. Similarly, the percentage of cool thermal energy storage for NPCM, against the dimensionless group, $FoSte^{1/3}Ra^{1/4}x^{1/4}$, is depicted in Fig. 8.

$$TECS = 1 - \left(1 - \frac{FoSte^{1/3}Ra^{1/4}x^{1/4}}{A}\right)^{B}\% \qquad (21)$$

With a maximum deviation of ±8% and A, B are constants given in Table 4.

Fig. 8 shows the variation of Nusselt number with time for different values of Rayleigh and Stefan numbers. It is noted that Nusselt number decreases as the time increases with significant effect of Rayleigh and Stefan numbers. As the time increases their effect decreases. Also, it is noted that, up to a certain value of Rayleigh number, the average Nusselt number increases with the decrease of Rayleigh number beyond this value it increases with the increase of Rayleigh number. So two correlations are deduced; one for Rayleigh number range $5.25 \times 10^{7} \leq Ra \leq 1.03 \times 10^{8}$ and having the form:

$$\frac{Nu}{Ra^{1/4}} = 10.732 e^{-0.025 FoSte^{1/3}Ra^{1/4}} \qquad (22)$$

The second correlation is deduced and illustrated in Fig. 8, for $Ra = 1.35 \times 10^{8}$ as:

$$\frac{Nu}{Ra^{1/4}} = 22.653 e^{-0.026 FoSte^{1/3}Ra^{1/4}} \qquad (23)$$

The average Nusselt number is correlated to the dimensionless group as shown in Fig. 8:

$$\frac{Nu}{Ra^{1/4}} = 25.844 e^{-0.034 FoSte^{1/3}Ra^{1/4}x^{1/4}}. \qquad (24)$$

The data in Fig. 9 is utilized to correlate the complete charging time to Rayleigh number in the form:

$$Fo = 27127 Ra^{-0.567} \qquad (25)$$

With a maximum deviation of ±3%.

The complete charging time for NPCM is correlated to Rayleigh number and illustrated in Fig. 9 as:

$$Fo = 98293.5 Ra^{-0.646} \qquad (26)$$

With a maximum error of ±12%; if the volume fraction of the nanoparticles is incorporated the correlation becomes:

$$Fo = 117112 Ra^{-0.6} x^{-0.1445} \qquad (27)$$

With a maximum error of ±10%. The figure shows that the increase of volume fraction of nanoparticles from 0.5% to 2% (increase by 400%) results in a decrease of the complete charging time by an average percentage of 19%. Also, the increase of Rayleigh number by 160% results in a decrease of total charging time by an average percentage of 49%. This shows that the complete charging time is more influenced by the Rayleigh number than that by the volume fraction and this indicated from the indices of Correlation Eq. (27). Also, the combined effect of increasing both the volume fraction of nanoparticles and Rayleigh number leads to a percentage reduction of about 59%. All results uncertainties are listed in Table 2.

6. Conclusions

From the discussions of the experimental results and on the freezing behavior of pure water as PCM and NPCM with different volume fraction up to 2% in a spherical geometry; the following conclusions can be drawn:

- For pure PCM an average percentage reduction of 43% of the complete charging time due to increase of Rayleigh number by 164%.
- The increase of the volume fraction of nanoparticles in the NPCM enhances the freezing process, i.e. increase the rate of freezing and reduce the total charging time by about 19% for volume fraction of 2%.
- About 49% percentage reduction of the complete freezing (charging) time for NPCM is observed due to increasing Rayleigh number by 160% and total reduction in the charging time by 59% by the increase of Rayleigh number and volume fraction of 2%.
- The enhancement of heat transfer during the freezing process is more influenced by Rayleigh number than that by the volume fraction.
- The calculations of Stefan and Rayleigh number showed that: Stefan number increases with the increase of volume fraction of nanoparticles and Rayleigh number decreases with increase of volume fraction.
- Useful empirical correlations for the solidified mass fraction, percentage of thermal energy cool storage and the average Nusselt number are obtained and can be helpful in practice.

References

[1] K.T. Adref, I.W. Eames, Experiments on charging and discharging of spherical thermal (ice) storage elements, Int. J. Energy Res. 26 (2002) 949–964.

[2] M. Cheralathan, R. Velraj, S. Renganarayanan, Performance analysis on industrial refrigeration system integrated with encapsulated PCM-based cool thermal energy storage system, Int. J. Energy Res. 31 (2007) 1398–1413.

[3] J.P. Bedecarrats, F. Strub, B. Falcon, J.P. Dumas, Phase change energy storage using spherical capsules: of a test plant, Int. J. Refrig. 19 (1996) 187–196.

[4] I.W. Eames, K.T. Adref, Freezing and melting of water in spherical enclosures of the type used in thermal (ice) storage system, Appl. Therm. Eng. 22 (2002) 733–745.

[5] K.A.R. Ismail, J.R. Henriquez, T.M. da Silva, A parametric study on the formation inside a spherical capsule, Int. J. Therm. Sci. 42 (2003) 881–887.

[6] C.W. Chan, F.L. Tan, Solidification inside a sphere- an experimental study, Int. Commun. Heat Mass Transf. 33 (2006) 335–341.

[7] K.A.R. Ismail, R.I.R. Moraes, A numerical and experimental investigation of different containers and PCM options for cold storage modular units for domestic applications, Int. J. Heat Mass Transf. 52 (2009) 4195–4202.

[8] R.I. ElGhanam, R.A. Abdelaziz, M.H. Sakr, H.E. Abdelrhman, An experimental study of freezing and melting of water inside spherical capsules used in thermal energy storage systems, Ain-Shams Eng. J. 3 (2012) 33–48.

[9] Shuying Wu, Dongsheng Zhu, Xinfang Li, Hua Li, Junxi Lei, Thermal energy storage behavior of Al_2O_3-H_2O nanofluids, Thermochimica Acta 483 (2009) 73–77.

[10] V. Kumaresam, P. Chandrasekaran, M. Nada, A.K. Maini, R. Velraj, Role of PCM based nanofluids for energy efficient cool thermal storage system, Int. J. Refrig. 36 (2013) 1641–1647.

[11] P. Chandrasekaran, M. Cheralathan, V. Kumaresan, R. Velraj, Enhanced heat transfer characteristics of water based copper oxide nanofluid PCM in a spherical capsule during solidification for energy efficient cool thermal storage system, Energy 72 (2014) 636–642.

[12] A.O. Elsayed, Numerical study on performance enhancement of solid-solid phase change materials by using multi-nanoparticles mixture, J. Energy Storage 4 (2015) 106–112.

[13] A.A. Altohamy, M.F. Abd Raboo, R.Y. Sakr, A.A.A. Attia, Effect of water based Al_2O_3 nanoparticles PCM on cool storage performance, Appl. Therm. Eng. 84 (2015) 331–338.

[14] A.A.A. Attia, A.A. Altohamy, M.F. Abd Raboo, R.Y. Sakr, Comparative study on Al_2O_3 nanoparticles addition on cool storage performance, Appl. Therm. Energy 94 (2016) 449–457.

[15] E. Assis, L. Katsman, G. Ziskind, R. Letan, Numerical and experimental study of melting in a spherical shell, Int. J. Heat Mass Transf. 50 (2007) 1790–1804.

[16] L.W. Fan, Z.Q. Zhu, Y. Zeng, Q. Ding, M.J. Liu, Unconstrained melting heat transfer in spherical container revisited in the presence of nano-enhanced phase change material NePCM, Int. J. Heat Mass Transf. 95 (2016) 1057–1069.